

This article was downloaded by:

On: 25 January 2011

Access details: Access Details: Free Access

Publisher Taylor & Francis

Informa Ltd Registered in England and Wales Registered Number: 1072954 Registered office: Mortimer House, 37-41 Mortimer Street, London W1T 3JH, UK



Separation Science and Technology

Publication details, including instructions for authors and subscription information:

<http://www.informaworld.com/smpp/title~content=t713708471>

Fluid Flow Characteristics of Forced Flow Electrophoresis

Hwa-Won Ryu^{ab}; Milan Bier^a

^a CENTER FOR SEPARATION SCIENCE UNIVERSITY OF ARIZONA, TUCSON, ARIZONA ^b

Department of Chemical Engineering, Chonnam National University, Kwangju, Korea

To cite this Article Ryu, Hwa-Won and Bier, Milan(1990) 'Fluid Flow Characteristics of Forced Flow Electrophoresis', Separation Science and Technology, 25: 9, 1007 — 1020

To link to this Article: DOI: 10.1080/01496399008050381

URL: <http://dx.doi.org/10.1080/01496399008050381>

PLEASE SCROLL DOWN FOR ARTICLE

Full terms and conditions of use: <http://www.informaworld.com/terms-and-conditions-of-access.pdf>

This article may be used for research, teaching and private study purposes. Any substantial or systematic reproduction, re-distribution, re-selling, loan or sub-licensing, systematic supply or distribution in any form to anyone is expressly forbidden.

The publisher does not give any warranty express or implied or make any representation that the contents will be complete or accurate or up to date. The accuracy of any instructions, formulae and drug doses should be independently verified with primary sources. The publisher shall not be liable for any loss, actions, claims, proceedings, demand or costs or damages whatsoever or howsoever caused arising directly or indirectly in connection with or arising out of the use of this material.

Fluid Flow Characteristics of Forced Flow Electrophoresis

HWA-WON RYU* and MILAN BIER†

CENTER FOR SEPARATION SCIENCE
UNIVERSITY OF ARIZONA
TUCSON, ARIZONA 85721

Abstract

Fluid flow in forced flow electrophoresis has not been previously analyzed, even though it presents some interesting aspects. The effectiveness of this method for biological separations is due to a superimposition of an electric field on filtration. A mathematical model is presented, describing fluid flow and mass transfer for dilute solutions at electrical potentials less than the critical one. The calculated solute trajectories in a channel are determined by the ratio of the electrophoretic velocity to the withdrawal velocity through the permeable wall. The stationary layer and the layer in which all the solutes arrive at the permeable membrane at the end of the channel are also calculated. The concentration of the filtrate through the permeable membrane is obtained from the material balance of the solute entering the channel. Increased performance is obtained by means of a double-stage forced flow electrophoresis, where the ratio of final filtered solute concentration to inlet concentration is shown to be the square of the same ratio at the first stage.

INTRODUCTION

In the present paper we wish to present a mathematical model describing flow characteristics and mass transfer believed to prevail in an input channel in forced flow electrophoresis (FFE). FFE is the method used for the isolation of lectins from the extract of lentils (*Lens culinaris*), as presented in a companion paper in this *Journal* (1). FFE was developed by Bier (2) and has been applied to a wide range of separation problems, ranging from electrofiltration of clay suspensions (3) to *in-vivo* isolation of immuno-

*Permanent address: Department of Chemical Engineering, Chonnam National University, Kwangju, Korea.

†To whom correspondence should be addressed.

globulins from blood maintained in extracorporeal circulation (4). These applications have been reviewed previously (2).

The apparatus for FFE comprises one or more flow-through cells, each cell being subdivided in two compartments by means of a protein-permeable filter. Part of the process fluid is forced through the filter, the applied electrical field causing retardation of mass transfer of electrically charged particles or solutes of proper polarity. Thus, the feed is separated into two fractions: the filtered effluent, containing mainly proteins close to their isoelectric point, and the residual feed, concentrated but impoverished of the isoelectric components. FFE is capable of high throughput by using multiple cells of large filter area, arranged in parallel between a single pair of electrodes. This study is a continuation of use of lectin proteins as a model system for large-scale electrophoresis (5).

In our effort to utilize the method for the isolation of lentil lectins (1), we have obtained substantially higher purity of the isoelectric proteins by using a double-stage modification of FFE. The computed flow characteristics and concentration profiles at various operational parameters clearly show the advantages of the double-stage FFE over the single stage. In the derivation it was assumed that the desired product is at its isoelectric point and that the undesired proteins are acidic and therefore negatively charged. The model differs from the usual one for electrofiltration since all the solutes were assumed to be permeable to one of the membranes. Some similarities of FFE with Giddings (6) field-flow fractionation (FFF) will become obvious.

MODELING OF FORCED FLOW ELECTROPHORESIS

The arrangement of the FFE is illustrated schematically in Fig. 1. Each electrophoretic cell is defined by membranes which do not allow passage of macromolecular proteins but are fully permeable to buffering ions, and are subdivided into two subcompartments by filters. The protein solution is continuously fed through the left, input, compartment, and part of it is forced through the filter by a metering pump. The electrical field is applied perpendicularly to the filter, causing all negatively charged proteins or solutes to migrate to the left while isoelectric or positively charged components migrate to the right. Details of cell construction can be found elsewhere, together with alternate membrane-filter arrangements (2, 7). The axial velocity profile in the channel shown in Fig. 2 can be expressed by the following parabolic equation:

$$v_x = 6\langle v_x \rangle \left(\frac{y}{B} \right) \left(1 - \frac{y}{B} \right) \quad (1)$$

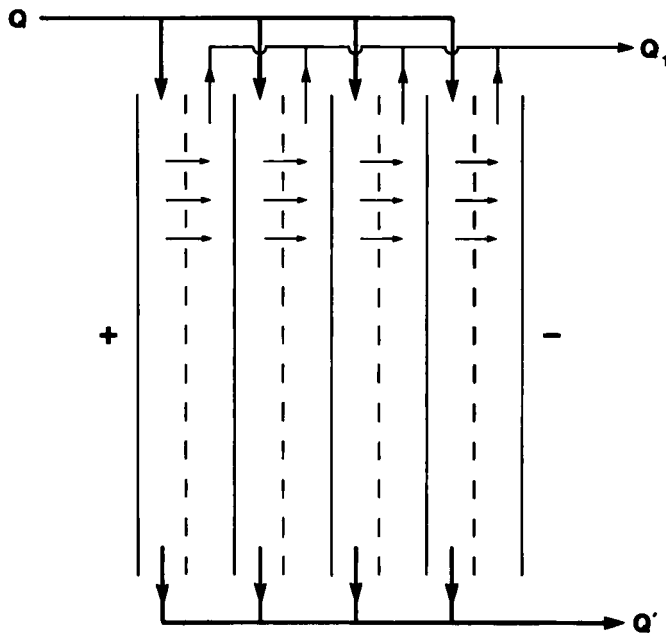


FIG. 1. Schematic representation of a usual single-stage FFE. (Q = feed, Q' = residual feed, Q_1 = isoelectric component, (—) macromolecule-impermeable membrane, (--) macromolecule-permeable membrane.)

where $\langle v_x \rangle$ is the average axial velocity over the cross section of the channel and B is the channel width. The transverse flow velocity profile in a channel can be obtained by assuming that the velocity through the porous wall, v_w , is very small compared to the mean velocity in the channel and is constant throughout the porous wall. The channel width is assumed to be sufficiently large so that the velocity variation in the z -direction can be neglected. The continuity equation for a fluid with constant density is

$$\frac{\partial v_x}{\partial x} + \frac{\partial v_y}{\partial y} = 0 \quad (2)$$

Inserting Eq. (1) in Eq. (2) and integrating with respect to y , we get

$$v_y = -6 \frac{d\langle v_x \rangle}{dx} \int \left[\left(\frac{y}{B} \right) - \left(\frac{y}{B} \right)^2 \right] dy \quad (3)$$

During integration the constant is made zero from the no-slip boundary condition at $y = 0$. The average axial velocity in the channel varies linearly

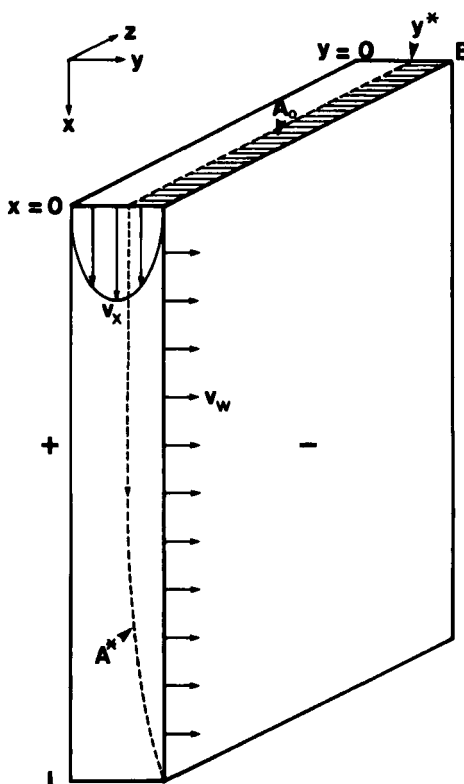


FIG. 2. Modeling of fluid flow in an FFE channel. (Left wall: macromolecule-impermeable membrane; right wall: macromolecule-permeable membrane.)

as in the following equation, due to the constant v_w :

$$\langle v_x \rangle = \langle v_x \rangle_0 - \frac{x}{B} v_w \quad (4)$$

Therefore the final expression for the transverse velocity in a channel can be expressed as

$$v_y = v_w \left[3 \left(\frac{y}{B} \right)^2 - 2 \left(\frac{y}{B} \right)^3 \right] \quad (5)$$

The above equation is the same as the one derived by Giddings (8). In the case where the electrical field, E , is applied in the negative y -direction,

the net velocity of a solute, v_{ys} , which has a mobility of μ , can be written as

$$v_{ys} = v_w \left[3 \left(\frac{y}{B} \right)^2 - 2 \left(\frac{y}{B} \right)^3 \right] - \mu E \quad (6)$$

Therefore, if the transverse velocity induced by suction through the filter is smaller than the electrophoretic velocity toward the anode, or $v_y < v_e = \mu E$, all the negatively charged proteins will migrate toward the left impermeable membrane and will be separated from the positively charged as well as the isoelectric proteins. The transverse velocity, however, is not constant and varies with y so that there exists a position where net solute velocity is zero at a specific value of v_e/v_w . The position of this stationary layer, y_s , is defined as the y -position at the inlet of a protein which has a net zero y -velocity in the channel and is determined by

$$3 \left(\frac{y_s}{B} \right)^2 - 2 \left(\frac{y_s}{B} \right)^3 = \frac{v_e}{v_w} \quad (7)$$

To meet the $0 \leq (y_s/B) \leq 1$ condition, v_e/v_w should be in the range of $0 \leq (v_e/v_w) \leq 1$. y_s can be easily calculated by using the Newton-Raphson method and is presented in Fig. 3. It should be noted that y_s does not depend on L/B or $v_w/\langle v_x \rangle_0$ but depends only on the ratio of v_e/v_w . The trajectories of solutes (proteins) in a channel can be calculated by inte-

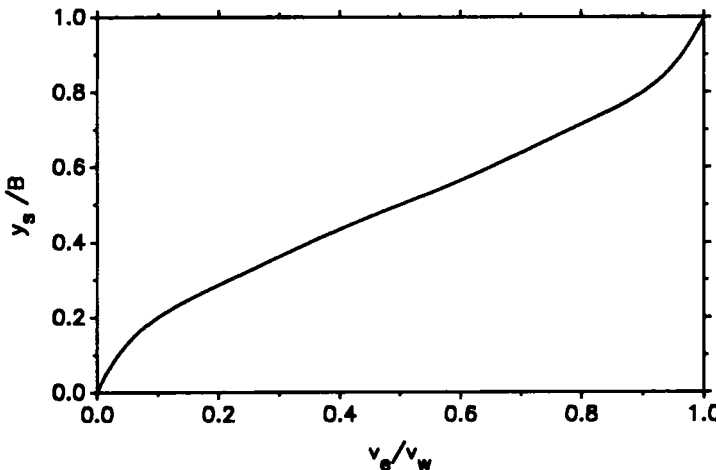


FIG. 3. Position of a stationary layer.

grating the axial and transverse velocities with time as follows:

$$x = x_0 + 6\langle v_x \rangle \int_0^t \left[\left(\frac{y}{B} \right) - \left(\frac{y}{B} \right)^2 \right] dt \quad (8)$$

$$y = y_0 + \int_0^t \left\{ v_w \left[3 \left(\frac{y}{B} \right)^2 - 2 \left(\frac{y}{B} \right)^3 \right] - v_e \right\} dt \quad (9)$$

The integration, however, is not easy because $\langle v_x \rangle$ in Eq. (8) depends on x in accordance with Eq. (4) and because the time-dependent variable y in Eq. (9) is expressed in an implicit form. The solution is obtained with the Runge-Kutta method of order four. Typical trajectories of solutes in a channel are shown in Fig. 4 in the case where $v_w/\langle v_x \rangle_0 = 0.01$, $L/B = 2.0$, and $v_e/v_w = 0.2, 0.5$, and 1.0 , respectively. The critical voltage in electrofiltration is defined as the voltage at which a balance exists between the particle flow velocity and the electrophoretic velocity (2). The same

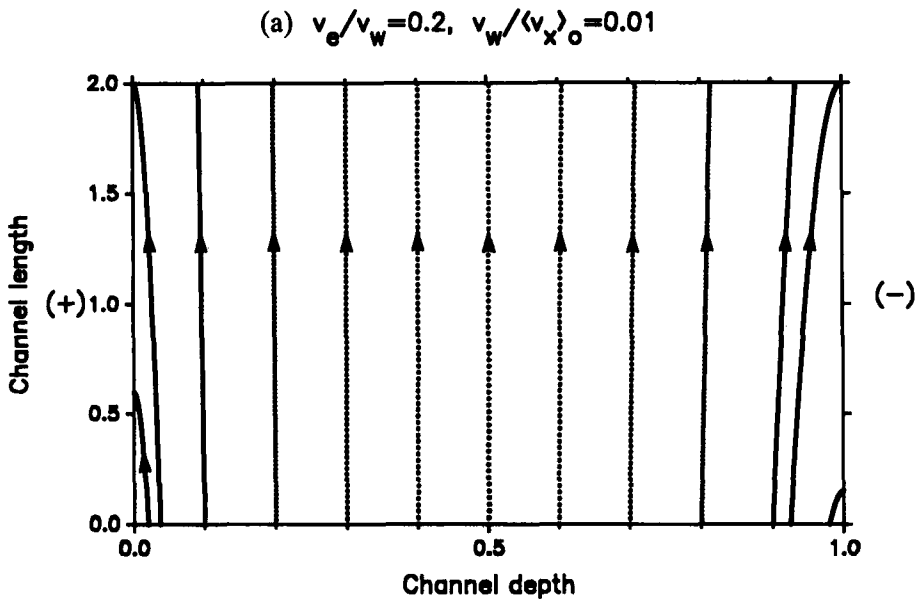
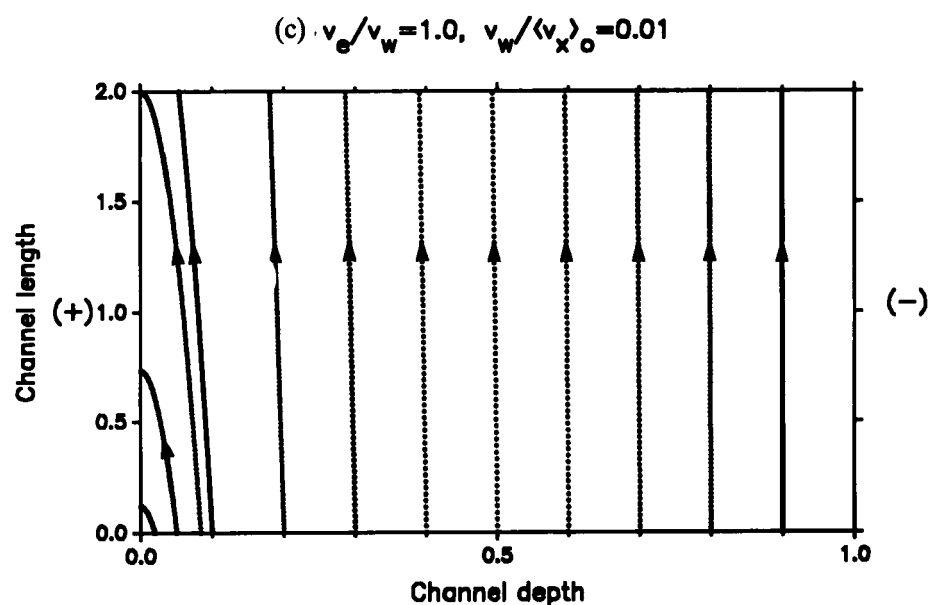
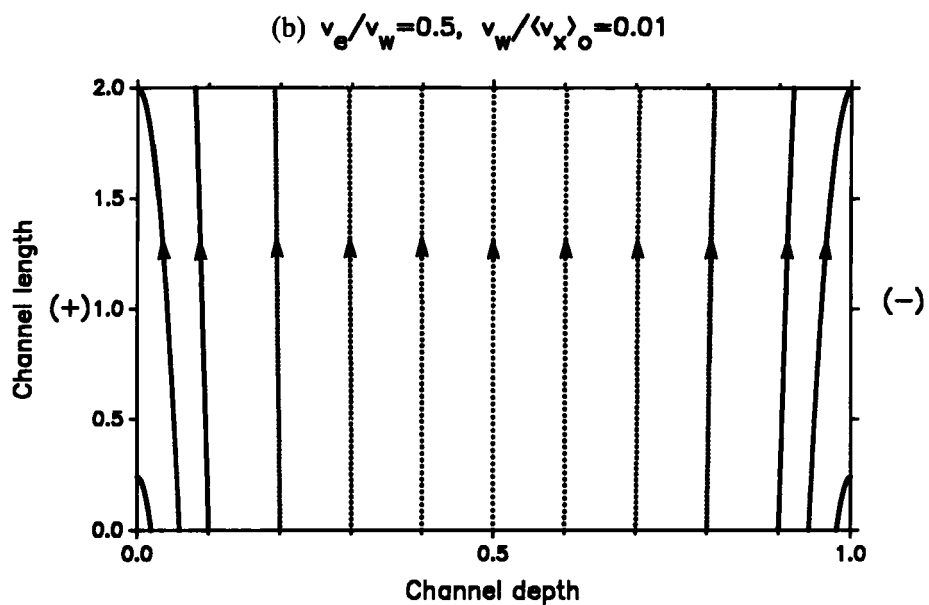


FIG. 4. Pathlines of solutes in a channel. (a) $v_e/v_w = 0.2$, $v_w/\langle v_x \rangle_0 = 0.01$. (b) $v_e/v_w = 0.5$, $v_w/\langle v_x \rangle_0 = 0.01$. (c) $v_e/v_w = 1.0$, $v_w/\langle v_x \rangle_0 = 0.01$. (Flow direction: Bottom to top. The channel length and the channel depth are nondimensionalized after being divided by the maximum channel depth B .)



concept can be employed here so that at a critical voltage the net transverse velocity of a solute at the permeable membrane is zero. Therefore, the critical voltage, E_c , can be written as

$$E_c = v_w / \mu \quad (10)$$

At a voltage lower than E_c the stationary layer will exist in the channel, as mentioned above, and at a voltage higher than E_c a clear boundary layer will develop in the channel near the permeable membrane (9). The stationary layer divides the channel into two regions so that solutes to the left of this plane will move toward the anode but solutes at the right will move toward the cathode. Since the solutes in the middle of the channel have a large axial velocity compared to the transverse velocity, they will pass through the channel and will not arrive at either of the walls, as shown in Fig. 4. However, solutes close to one of the walls have a lower axial velocity and thus have a longer residence time, and are therefore more likely to arrive at one of the walls.

Let us define t_w as the residence time of a solute which meets one of the walls and x_w as the axial distance from the entrance to the position at which a solute meets one of the walls after t_w . Both t_w and x_w can be obtained

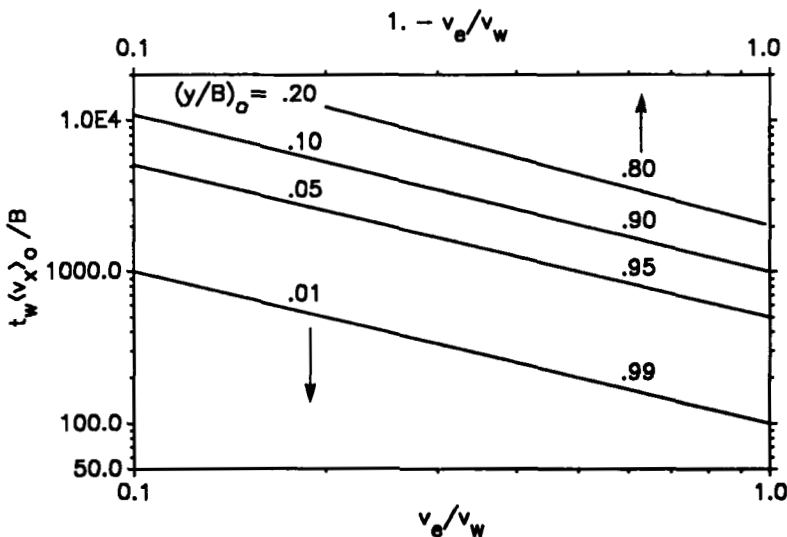


FIG. 5. Residence time of a solute which is added near one of the walls.

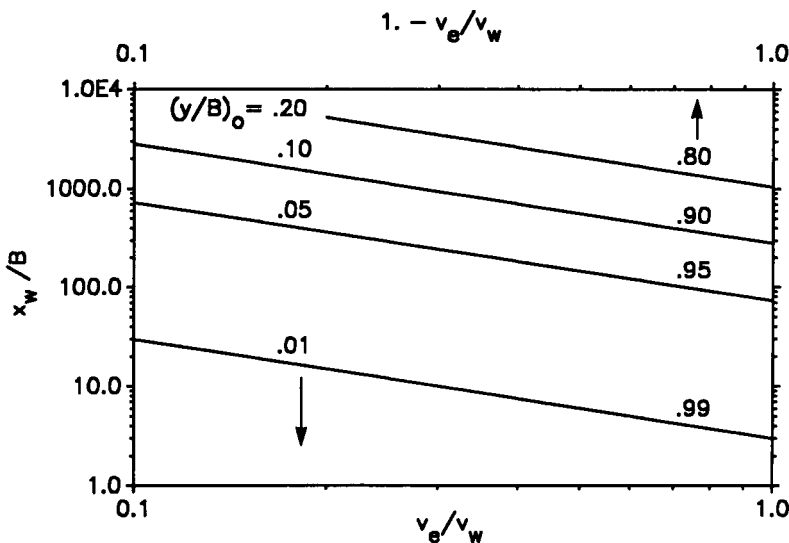


FIG. 6. Axial distance from inlet to the position where a solute flows through the permeable wall.

from Eq. (8) and Eq. (9) and are shown in Figs. 5 and 6. Both of them are linearly dependent on both the velocity ratio v_e/v_w and the dimensionless inlet y -position of a solute, $(y/B)_0$, adjacent to one of the walls. But the solutes which enter near the middle of the channel will have very large t_w and x_w . Particularly in the case of $(y/B)_0 = (y_s/B)$, t_w and x_w will be infinite, therefore these regions are not shown in the figures. Let us define y^* as the inlet fluid layer whose solutes can reach the permeable wall at the end of the channel or at $(x, y) = (L, B)$. Figure 7 shows that y^* is proportional to the velocity difference $(v_w - v_e)$. The fraction of inlet volumetric flow rate, F , in which solutes come out through the permeable wall can be calculated

$$F = \frac{\int_y^B v_x dy}{\int_0^B v_x dy} \quad (11)$$

$$= 1 - 3 \left(\frac{y^*}{B} \right)^2 + 2 \left(\frac{y^*}{B} \right)^3 \quad (12)$$

The average concentration of a solute that comes through a permeable wall can be calculated from the material balance for solutes which enter

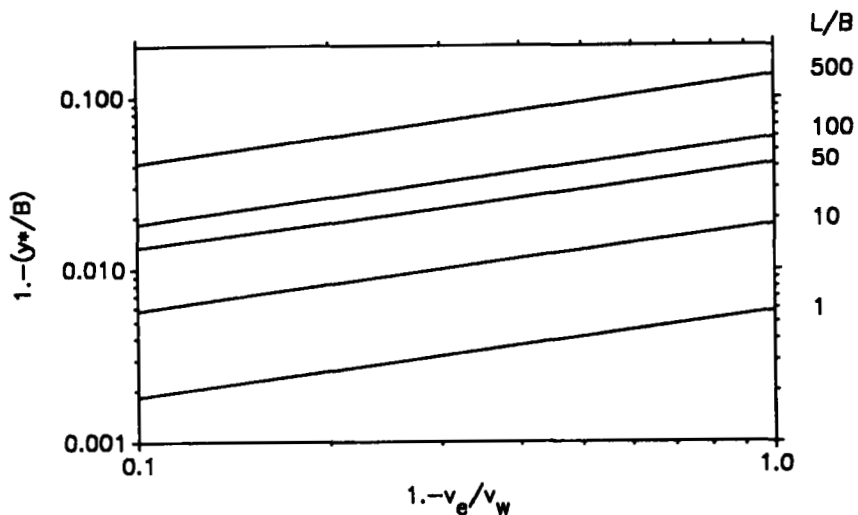


FIG. 7. Inlet position of a solute layer in which a solute will come out through the permeable membrane at the channel exit.

between the layer of $y = y^*$ and $y = B$. Namely,

$$\iint_{A^0} cv_x dA = \iint_{A^*} D \frac{\partial c}{\partial y} dA + \iint_{A^w} cv_y dA - A_w \left(D \frac{\partial c}{\partial y} \Big|_{y=B} \right) \quad (13)$$

Therefore the average concentration through the filter can be expressed as

$$\langle c_w \rangle = \frac{c_0}{v_w L} \int_{y^*}^B v_x dy - \frac{1}{v_w A_w} \iint_{A^*} D \frac{\partial c}{\partial y} dA + \frac{1}{v_w} \left(D \frac{\partial c}{\partial y} \Big|_{y=B} \right) \quad (14)$$

where c_0 is the inlet concentration. The ratio of the outlet to inlet concentration is obtained for the case in which the diffusion terms can be ignored compared to the convectional mass transfer in Eq. (14). Or,

$$\frac{\langle c_w \rangle}{c_0} \approx \frac{\langle v_x \rangle_0}{v_w} \frac{B}{L} \left[1 - 3 \left(\frac{y^*}{B} \right)^2 + 2 \left(\frac{y^*}{B} \right)^3 \right] \quad (15)$$

By combining Eqs. (12) and (15),

$$\frac{\langle c_w \rangle}{c_0} \approx \frac{\langle v_x \rangle_0}{v_w} \frac{B}{L} F \quad (16)$$

The mass flux through the filter can be expressed by the following equation which is composed of both diffusion and convection:

$$N_y \Big|_{y=B} = -D \frac{\partial c}{\partial y} \Big|_{y=B} + (cv_y) \Big|_{y=B} \quad (17)$$

$$= \frac{c_0}{L} \int_{y^*}^B v_x dA - \frac{1}{A_w} \iint_{A^*} D \frac{\partial c}{\partial y} dA \quad (18)$$

Therefore, the average concentration in a channel at the exist can be calculated from

$$\langle cv_x \rangle|_{x=L} = c_0 \langle v_x \rangle_0 - \frac{1}{B} \int_0^L N_y|_{y=B} dx \quad (19)$$

$$= c_0 \langle v_x \rangle_0 - \frac{c_0}{BL} \int_0^L \int_{y^*}^B v_x dy dx - \frac{1}{A_w B} \int_0^L \left[\iint_{A^*} D \frac{\partial c}{\partial y} dA \right] dx \quad (20)$$

The situation is different in a double mode operation, the case where the outflow through the permeable membrane is fed to the next channel. The average concentration of throughput will be expressed as follows by assuming a perfect mixing just before entering the second stage:

$$\langle c_w \rangle_2 = \frac{\langle c_w \rangle_1}{v_w L} \int_{y^*}^B v_x dy - \frac{1}{v_w A_w} \iint_{A^{**}} D \frac{\partial c}{\partial y} dA + \frac{1}{v_w} \left(D \frac{\partial c}{\partial y} \Big|_{y=B^{**}} \right) \quad (21)$$

where ** means the control surface at the second stage and subscripts 1 and 2 represent output concentration from the 1st and 2nd stage, respectively. Here again we can get an approximate average concentration by ignoring the diffusion terms:

$$\langle c_w \rangle_2 \approx \frac{c_0}{(v_w L)^2} \left(\int_{y^*}^B v_w dy \right)^2 \quad (22)$$

or

$$\frac{\langle c_w \rangle_2}{c_0} \approx \left(\frac{\langle c_w \rangle_1}{c_0} \right)^2 \quad (23)$$

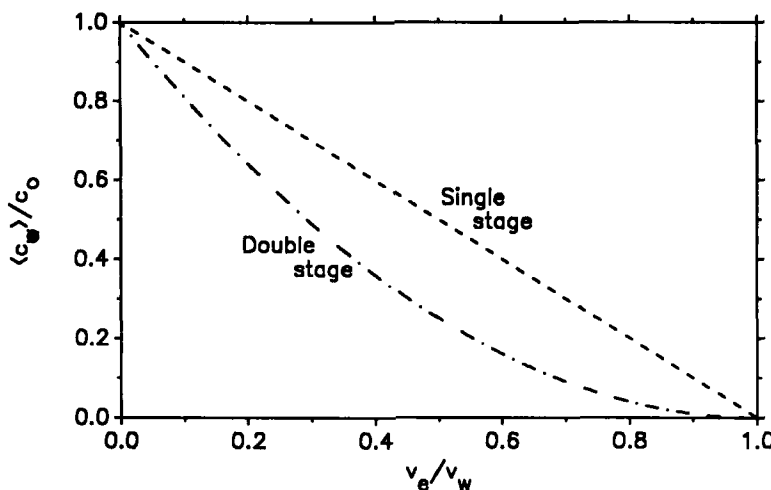


FIG. 8. Average concentration of exit solution from permeable wall.

Both $\langle c_w \rangle_1$ and $\langle c_w \rangle_2$ are shown in Fig. 8. Since the ratio of $\langle c_w \rangle_1 / c_0$ is much smaller than 1 in the usual polarization mode, the outlet solution from the second stage is highly purified.

DISCUSSION

To the best of our knowledge, no previous model of FFE has been presented. The method combines the effects of electrophoresis and filtration and bears some similarities to field-flow fractionation (FFF), introduced by Giddings (10). In FFE, part of the process fluid is forced through a macromolecule-permeable barrier, a filter, and the electric field retarding the transport through the filter of electrically charged solutes or particles of suitable polarity, but permitting the filtration of uncharged solutes. In FFF, differential retardation is achieved by applying a force field, such as gravity (11), flow (12), electrical (13), or temperature gradient (14), in a direction normal to a laminar flow between parallel plates or in capillaries. In hyperlayer FFF, the electrical or gravity field is combined with the flow field to exclude interactions between the sample components and the column walls (15). The main differences between FFE and FFF are: 1) FFE separates the feed solution or suspension into two fractions: the filtered effluent and the residual feed. FFF resembles conventional chromatographic separations in that solute or particle bands are retarded by the force field as they are developed and eluted from the flow channel. 2) FFE

takes advantage of macromolecules filtering through a membrane, while FFF uses macromolecule-impermeable membranes.

The model given here is only applicable to a well-cooled solution of low concentration, as we neglect changes of physical parameters during separation, such as viscosity, density, or electrical conductivity. Electroosmosis and gravitationally caused decantation are also neglected. In deriving Eq. (5) we started from the continuity equation, contrary to Giddings (8) who formulated it from macroscopic mass balance. In either case the axial velocity is assumed to be large enough so that it is not affected by the velocity through the permeable wall except that the average velocity is expressed in depletion form, as in Eq. (4). This is reasonable since the velocity ratio $v_w/\langle v_x \rangle_0$ in the usual FFE or FFF process is less than the order of 10^{-3} . From perturbation analysis, however, we have found that Eq. (1) and Eq. (5) are only zero-order perturbation solutions (16). In the plots of Fig. 5 through Fig. 8, such physical parameters as y^* , t_w , x_w , F , or $\langle c_w \rangle$ are shown to be mathematically linear in the range of this analysis.

CONCLUSION

Though our analysis does not represent a full explanation of the fluid flow and mass transport, we believe that it still gives the concept and advances the understanding of FFE. The derived model predicts the stagnant layer from Eq. (7) or Fig. 3, the trajectory of solutes from Eq. (8) and Eq. (9), the average concentration through the filter from Eq. (14), and the average concentration at the channel exit from Eq. (20). When FFE is operated in double stage, Eq. (23) shows that the ratio of impurity concentration in the final product to initial feed concentration will be about the square of the ratio obtainable from single-stage operation.

Acknowledgments

The authors acknowledge the support by the Korea Science and Engineering Foundation and by the NASA grant NAGW-693.

REFERENCES

1. M. Bier, T. Long and H.-W. Ryu, *Sep. Sci. Technol.*, **25**, 997 (1990).
2. M. Bier, in *Membrane Processes in Industry and Biomedicine* (M. Bier, ed.), Plenum, New York, 1971, p. 233.
3. S. P. Moulik, F. C. Cooper, and M. Bier, *J. Colloid Interface Sci.*, **24**, 427 (1967).
4. M. Bier, C. D. Beavers, W. G. Merriman, F. K. Merkel, B. Eiseman, and T. Z. Starzl, *Trans. Am. Soc. Artif. Intern. Organs*, **16**, 325 (1970).
5. P. Wenger, A. Heydt, N. B. Egen, T. D. Long, and M. Bier, *J. Chromatogr.*, **455**, 225 (1988).
6. J. C. Giddings, *Ibid.*, **470**, 327 (1989).
7. K. Hannig, in *Electrophoresis*, Vol. II (M. Bier, ed.), Academic, New York, 1967, p. 422.

8. J. C. Giddings, *Sep. Sci. Technol.*, **21**, 831 (1986).
9. Y. Liu, D. Gidaspow, and D. T. Wasan, *Part. Sci. Technol.*, **1**, 27 (1983).
10. J. C. Giddings, *Sep. Sci.*, **1**, 123 (1966).
11. J. C. Giddings and F. S. Yang, *J. Colloid Interface Sci.*, **105**, 55 (1985).
12. J. C. Giddings, F. J. Yang, and M. N. Myers, *Anal. Chem.*, **48**, 1126 (1976).
13. K. D. Caldwell, L. F. Kesner, M. N. Myers, and J. C. Giddings, *Science*, **176**, 296 (1972).
14. G. H. Thompson, M. N. Meyers, and J. C. Giddings, *Anal. Chem.*, **41**, 1219 (1969).
15. J. C. Giddings, *Sep. Sci. Technol.*, **18**, 765 (1983).
16. H.-W. Ryu, *Ind. Eng. Chem. Res.*, Submitted.

Received by editor November 6, 1989